Progress In Electromagnetics Research, PIER 50, 135–161, 2005

FORMULATION OF EMISSION FROM RELATIVISTIC FREE ELECTRONS IN A RING STRUCTURE FOR ELECTRO-OPTICAL APPLICATIONS

R. Sabry and S. K. Chaudhuri

Department of Electrical and Computer Engineering
University of Waterloo
Waterloo, Ontario, N2L 3G1, Canada

Abstract—A new scheme for high-speed electro-optical conversions with potential application to data communication is investigated. As the core of investigation, a ring model utilizing relativistic electrons is introduced and the operating characteristics such as coupled wavelengths, gain and power are derived for a circular type of interaction. Advantages are addressed and practical challenges associated with the realization of this conceptual scheme are discussed in light of advances in fundamentally similar relativistic free electron lasing schemes.

1. INTRODUCTION AND OBJECTIVES

There has been considerable effort to advance the state of coherent sources of radiation using relativistic electrons [1]. In the so-called free-electron lasers (FELs), wavelength of the emitted light is found by Doppler shifting the electron modulation frequency, i.e., $\lambda_L \approx \lambda_\Lambda/2\gamma^2$, where λ_Λ is the spatial periodicity of the electron modulation, $\gamma = (1-(v/c)^2)^{-1/2}$ is the relativistic energy of the electrons and, v is the center velocity of the electron beam. Conserving the main principle that is the interaction of high-energy electrons with the field (magnetic or electromagnetic) to create short wavelength emission, various configurations have been devised and realized. Among them are wiggler-type free-electron lasers [2–5], wiggler-free free-electron lasers and Orotron or Smith-Purcell free-electron lasers [6]. The steady progress in FEL generation of coherent radiation has been accompanied by advances in the electron injection technology [1, 7], to achieve high quality electron beam in terms of energy spread and brightness.

There has also been increasing growth in number and nature of usage of FELs radiation. Such radiations have been proven to be ideal for a vast variety of applications due to FELs tunability, short pulse length, synchronize operation, bandwidth and beam quality [1]. One class of applications are the research and experimentations in areas such as atomic physics, plasmas and nanoscale structures. Another potential class of applications are the ones with wide-bandwidth requirements.

Advances in Microsystems offer the possibility of downsizing the free-electron lasing scheme, and therefore, realization of such sources of coherent radiation in an economic and compatible size. Considering the described trend of progress in the technology and salient features of the FEL generators of violet and ultraviolet coherent radiation, it is reasonable to investigate the application of a similar scheme in high bit-rate data communication systems as an electro-optical modulator [8–11].

In this paper, we investigate a ring type of such interactions for data applications in two parts. Throughout the main part, the electro-optical coupling process is formulated to establish a theoretical frame of reference relating the operating characteristics (e.g., coupled wavelengths, gain, power) to the model key specifications (e.g., electron beam energy, EM modulation). In the second part; certain operating characteristics particular to this type of scenario such as bandwidth and tunability are described, effect of deviations from assumed or ideal model parameters such as energy spread are discussed, practical challenges and some potential solutions are addressed. These are

done by referring to the fundamentally similar FELs operations, reported achievements [12–29], and previously published work(s) such as dispersion analysis [8]. It should be noted that we cannot capture all aspects of a practical realization or the associated required assumptions to be included in the formulations. This is an insurmountable task that is ongoing challenge for the theoretical and experimental professionals in the area. The goal is to explore the potentials by formulating the key characteristics and basic physics. Effects of model elements uncertainty and deviation from ideal operation can be estimated from such formulations providing the underlying basic assumptions are valid.

The interaction model will be introduced in the next section and the cross-field requirements for guiding the electrons will be determined. In Section 3, the electro-optical coupling will be investigated through formulation of optical emission for certain field modulations. Section 4 will include discussions, practical challenges and conclusions.

2. INTERACTION MODEL

In the scheme proposed here, relativistic free-electrons are forced to travel along a circular path with a mean radius r_0 due to the action of a cross-field, i.e., perpendicular electric and magnetic fields. The cross-field requirements will be derived later in this section. Presence of a transversal electric/magnetic modulating field which is radially polarized with the azimuthal periodicity ϕ_Λ, causes the electrons to wiggle about their circular motion path. This results in a short-wavelength radiation which is strongly confined in a small cone around the circular or azimuthal direction of electrons' motion due to the so-called Bremsstrahlung phenomenon. Therefore, the laser emission is expected to be dominantly propagating in the azimuthal direction at a radius $r \approx r_0$ and be polarized in the radial direction (radiation gauge). These observations that are based on the basic physics of relativistic electron's interaction with radiation will be analytically confirmed in the next section. One advantage of this scheme is that electrons can be re-used for another interaction cycle. Another advantage is that for the same physical dimensions, this design offers a longer interaction length which results in the gain and power enhancement.

A view of the described interaction scenario utilizing relativistic electrons with circular trajectories is depicted as an interaction model in Figure 1. Assuming one-dimensional model in the transversal direction, dynamics of electrons are formulated in a cylindrical coordinate system (r, ϕ, z). The operating wavelength of the optical emission λ_L is determined by allowing these kinematics to interact

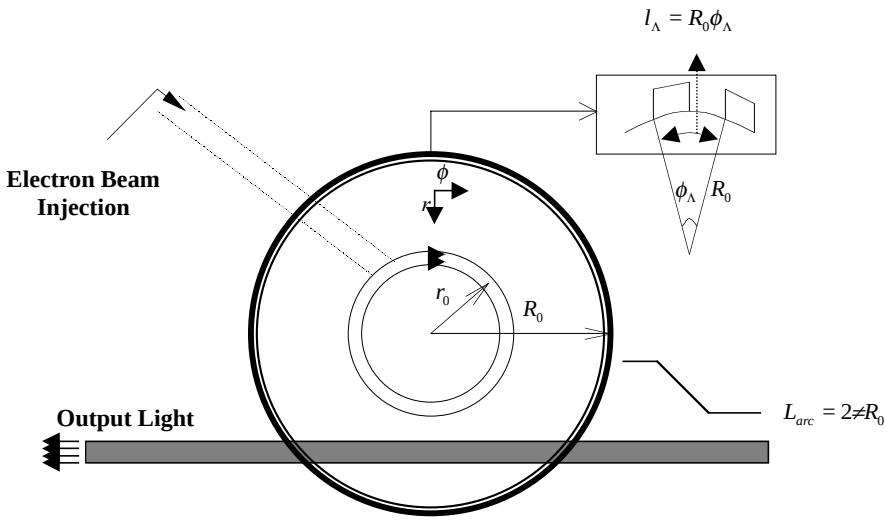

Figure 1. 2-dimensional model for the electro-optical modulator.

with the radiation. The latter is done by using the Lienard-Wiechert potentials that describe radiation from moving particles.

The high-energy electrons with the relativistic energy γ are injected into the interaction space and undergo a circular motion with a radius r_0 (mean radius associated with the electrons in the electron beam) under the influence of the cross-field and in the absence of modulating field. In the cylindrical coordinate system, the modulating static field has an azimuthal period ϕ_Λ and is located at a radius R_0. Electrons passing through interaction region execute N_Λ wiggles as a result of interaction with the respective modulating field which is radially polarized. As a result, an optical pulse with the wavelength λ_L is generated which tends to propagate in the azimuthal direction.

Therefore, it can be captured through coupling by a circular waveguide structure positioned in a close proximity of the electron beam. The wiggler arc length is given by:

$$L_{arc} = N_\Lambda \phi_\Lambda = 2\pi R_0 \tag{1}$$

Characteristics of the coherent or laser emission resulted from electron beam-field interaction are studied in the next section. First, however, it is necessary to investigate the cross-field requirements for the desired electron's circular motions (e.g., radius and angular velocity) which determine specifications of the output laser pulse.

2.1. Cross-Field Formulation

A relativistic electron moving in the (r, ϕ)-plane (2-dimensional interaction model) can be forced to undergo a circular motion by applying a cross-field configuration. This arrangement is formed through application of an uniform radial electric field $E_r^{(c)}$, and an uniform magnetic field in the z-direction $B_z^{(c)}$.

Motions of the high-energy electron with relativistic energy γ in the presence of the cross-field can be characterized by using the relativistic force equation:

$$\frac{d}{dt}(\gamma m \boldsymbol{v}) = e(\boldsymbol{E} + \boldsymbol{v} \times \boldsymbol{B}) \tag{2}$$

and the following kinematics equations:

$$\frac{d^2r}{dt^2} - r\left(\frac{d\phi}{dt}\right)^2 = \frac{e}{\gamma m}\left(E_r^{(c)} + rB_z^{(c)}\frac{d\phi}{dt}\right) \tag{3}$$

$$r\frac{d^2\phi}{dt^2} + 2\frac{d\phi}{dt}\frac{dr}{dt} = -\frac{e}{\gamma m}\left(B_z^{(c)}\frac{dr}{dt}\right) \tag{4}$$

Since we are interested in cyclotron motion of electrons at some angular velocity and/or angular frequency,

$$\frac{d\phi}{dt} = \omega_c = cte. \tag{5}$$

with a cyclotron radius r_0, (3), (4) can be simplified as:

$$\frac{d^2r}{dt^2} + r\left(\frac{d\phi}{dt}\right)^2 = \frac{e}{\gamma m}E_r^{(c)} \tag{6}$$

$$2\frac{d\phi}{dt} = -\frac{e}{\gamma m}B_z^{(c)} \tag{7}$$

Equations (6), (7) indicate that by choosing the cross-field components $E_r^{(c)}$ and $B_z^{(c)}$, circular motion of the relativistic electron can be characterized in terms of the cyclotron radius r_0 and cyclotron frequency $\omega_c = \frac{d\phi}{dt}$. Thus, we can determine the cross-field components for a desired circular motion. Since the prime purpose of the cross-field application is to create certain radius for the cyclotron motion of the relativistic electrons, it appears that there is no particular constraint on the cyclotron frequency ω_c and, therefore, there is one degree of freedom in determination of the required cross-field from (6), (7).

However, considering the fundamental mechanism of relativistic free-electron's emission in the direction of electron's motion on which the present interaction scheme is based, we require that the electrons be relativistic in the azimuthal direction, i.e., radial momentum be small compared with the azimuthal momentum ($p_\phi \gg p_r$). Accordingly, $p_\phi = \gamma m r_0 \frac{d\phi}{dt} \approx \gamma mc$. Thus,

$$r_0 \frac{d\phi}{dt} \approx c \tag{8}$$

and the cyclotron frequency can not be chosen arbitrarily. Application of (8) in (6) and (7) assuming $\frac{d^2r}{dt^2}/r \ll 1$ yields:

$$B_z^{(c)} = -\frac{2\gamma mc}{er_0} \tag{9}$$

$$E_r^{(c)} = \frac{\gamma mc^2}{er_0} \tag{10}$$

Applying (10), one can show that,

$$\frac{\delta r}{r_0} = \frac{er_0 E_r^{(c)}}{\gamma mc^2} \tag{11}$$

Equation (11) indicates that for a fixed cross-field arrangement, variations of the electron energy results in the change in the cyclotron radius r_0. This should be taken into the considerations when designing the interaction parameters.

3. LASER FIELD

To characterize the short-wavelength radiation associated with the described interaction scheme, the single-electron phase must be formulated through kinematic considerations.

Mechanism of lasing or coherent radiation is similar to the spontaneous emission. However, electrons develop a new phase due to their interaction with each other and with the radiation field and form bunches which are spaced a wavelength apart. As a result of this spatial bunching, the radiation from individual electrons add coherently and amplifies the laser field. To describe the transition toward coherent state, electron's behaviour in the process of interaction with the laser field are characterized.

3.1. Electron Kinematics

We assume a radially polarized modulating or electric/magnetic field is distributed along the circumference of a ring with the radius R_0 with N_Λ number of gratings and with the grating period l_Λ, i.e., $N_\Lambda l_\Lambda = 2\pi R_0$ or

$$N_\Lambda \phi_\Lambda = 2\pi \tag{12}$$

where ϕ_Λ is the angular or azimuthal period of the static modulating field. Observing from the electron's reference frame, the electrons experience effects of the modulating field through an interaction length of:

$$L = N_\Lambda \lambda_\Lambda \tag{13}$$

where

$$\lambda_\Lambda = r_0 \phi_\Lambda \tag{14}$$

The length λ_Λ can be viewed as the spatial period of the modulating field seen by the electrons.

Adopting an one-dimensional model in the transversal plane (r, z), the vector potential associated with the magnetic wiggler field seen by the relativistic electrons can be written as:

$$\begin{aligned} \boldsymbol{A}_\Lambda &= \sqrt{2} A_\Lambda \sin(K_{\phi\Lambda}\phi)\hat{r} \quad 0 < \phi < 2\pi \\ &= 0 \qquad\qquad\qquad\qquad\quad \text{otherwise} \end{aligned} \tag{15}$$

where $K_{\phi\Lambda} = \frac{2\pi}{\phi_\Lambda}$ is the static field's azimuthal wavenumber, A_Λ is the rms electric vector potential. It can be seen that electrons execute N_Λ wiggles as they travel through the interaction cycle.

Similarly, one gets for the electric wiggler field seen by the relativistic electrons,

$$\begin{aligned} \boldsymbol{E}_\Lambda &= \sqrt{2} E_\Lambda \sin(K_{\phi\Lambda}\phi)\hat{r} \quad 0 < \phi < 2\pi \\ &= 0 \qquad\qquad\qquad\qquad\quad \text{otherwise} \end{aligned} \tag{16}$$

where E_Λ is the rms electric field. Amplitude of the modulating electric field is assumed to be constant within the interaction space, i.e., $E_\Lambda = cte$.

Next step to formulate the particle or electron kinematics is to apply the relativistic force equation (2). Assuming invariance in the z direction, one can set $p_z = v_z = 0$ where $\boldsymbol{p}$ denotes the vector electron momentum. Neglecting effects of laser or radiation field on the particles to derive the resonant kinematics and using $\boldsymbol{B}_\Lambda = \nabla \times \boldsymbol{A}_\Lambda$, one finds:

$$\begin{aligned} \gamma m \frac{dv_r}{dt} &= -e \frac{d\phi}{dt} \frac{dA_r}{d\phi} \\ &= -e \frac{dA_r}{dt} \end{aligned} \tag{17}$$

Thus:

$$v_r = -\sqrt{2}\frac{c}{\gamma}a_\Lambda \sin(K_{\phi\Lambda}\phi) \tag{18}$$

where the dimensionless vector potential is given by:

$$a_\Lambda = \frac{eA_\Lambda}{mc} \tag{19}$$

Using the relativistic Hamiltonian in a cylindrical coordinate system:

$$\gamma mc^2 = \left((mc^2)^2 + c^2\left(p_r^2 + p_\phi^2\right)\right)^{1/2} \tag{20}$$

where $p_r = \gamma m v_r$, $p_\phi = \gamma m v_\phi$, and considering the approximation based on the design objective, i.e., $p_\phi \gg p_r$, we find:

$$\frac{d}{d\phi}(p_\phi p_r) \approx p_\phi \frac{dp_r}{d\phi} \tag{21}$$

For the electric modulating field (16), the force equation becomes:

$$\gamma m \frac{dv_r}{dt} = e(\boldsymbol{E}_\Lambda)\cdot \hat{r} \tag{22}$$

Where (21) yields,

$$v_r \approx \sqrt{2}\frac{c}{\gamma}e_\Lambda \sin(K_{\phi\Lambda}\phi) \tag{23}$$

and

$$e_\Lambda = \frac{r_0 e E_\Lambda}{mc^2 K_{\phi\Lambda}} \tag{24}$$

is the dimensionless electric field.

Making use of (18), we obtain the magnetic wiggler field modulation:

$$p_\phi = \gamma m v_\phi \approx \gamma mc\left\{1 - \frac{1}{2\gamma^2}\left[1 + a_\Lambda^2 - a_\Lambda^2\cos(2K_{\phi\Lambda}\phi)\right]\right\} \tag{25}$$

Similarly, one gets the electric wiggler field modulation (23):

$$p_\phi = \gamma m v_\phi \approx \gamma mc\left\{1 - \frac{1}{2\gamma^2}\left[1 + e_\Lambda^2 - e_\Lambda^2\cos(2K_{\phi\Lambda}\phi)\right]\right\} \tag{26}$$

Examining (25)–(26), we observe:

$$\frac{r}{c}\frac{d\phi}{dt} = 1 + O\left(\frac{1}{\gamma^2}\right) \tag{27}$$

which is expected since we require that $r\frac{d\phi}{dt} \approx c$. Setting $r = r_0 + \delta r(\frac{v_r}{v\phi} \ll 1)$ and combining (27) and (18) we find:

$$\frac{d\delta r}{dt} \approx \sqrt{2}\frac{a_\Lambda}{\gamma K_{\phi\Lambda}} r_0 \cos(K_{\phi\Lambda}\phi) \ll 1 \tag{28}$$

Application of (28) introduces a major simplification to the derivations of angular motion because r can be substituted by r_0. Moreover, as long as the angular momentum $p_\phi = \gamma m r\frac{d\phi}{dt}$ has the correct form, this substitution introduces no error to the overall picture of interaction because the radial oscillations will be contained in the angular variations $\frac{d\phi}{dt}$. In other words, we simply set the observation point at $r = r_0$. Accordingly,

$$\frac{d\phi}{dt} \approx \frac{c}{r_0}\left\{1 - \frac{1}{2\gamma^2}\left[1 + g_\Lambda^2 - g_\Lambda^2\cos(2K_{\phi\Lambda}\phi)\right]\right\} \tag{29}$$

where $g_\Lambda = a_\Lambda$ for a magnetic field modulation and, $g_\Lambda = e_\Lambda$ for that of an electric field.

The angular velocity consists of a mean motion together with an azimuthal oscillation which causes a *figure-eight* motion and generates higher order harmonics. For $\gamma \gg 1$, the solution to (29) is given by:

$$\phi = \phi_0 + \phi' \tag{30}$$

where

$$\phi_0 = \frac{ct}{r_0}\left[1 - \frac{1 + g_\Lambda^2}{2\gamma^2}\right] \tag{31}$$

Also,

$$\frac{d\phi'}{dt} = \frac{c}{2\gamma^2 r_0} g_\Lambda^2 \cos(2K_{\phi\Lambda}(\phi_0 + \phi')) \tag{32}$$

Solving (32) by expanding the right-hand side to orders of $\frac{1}{\gamma}$, we find:

$$\phi' = \frac{g_\Lambda^2}{4\gamma^2 K_{\phi\Lambda}} \sin(2K_{\phi\Lambda}\phi_0) \tag{33}$$

Similarly, one can derive the solution for (18), (23) when taking into account the condition $r|_{K_{\phi\Lambda}\phi_0 = \frac{\pi}{2}} = r_0$ as:

$$r = r_0 + \sqrt{2} r_0 \frac{g_\Lambda}{\gamma K_{\phi\Lambda}} \cos(K_{\phi\Lambda}\phi_0) \tag{34}$$

3.2. Resonance

Resonant characteristics are derived by examining the conditions for stationary phase.

The overall phase is found by making use of the spectral fluence associated with the emitted radiation [9–11]. Accordingly, the phase is associated with the integrand:

$$Int = \boldsymbol{n} \times (\boldsymbol{n} \times \boldsymbol{v}) \exp[j(\omega_L t - K_L \boldsymbol{n} \cdot \boldsymbol{r})] \tag{35}$$

where

$$\omega_L = \frac{c}{r_0} K_{\phi L} \tag{36}$$

is the angular frequency and

$$K_{\phi L} = \frac{2\pi}{\phi_L} \tag{37}$$

is the angular wavenumber associated with the emitted light observed at the radius r_0 and, ϕ_L denotes the azimuthal or angular period of the light. Thus:

$$\lambda_L = \frac{2\pi}{K_L} = r_0 \phi_L \tag{38}$$

is the light wavelength. In (35), the unit vector $\boldsymbol{n}$ in the direction of emission is given by:

$$\boldsymbol{n} = \sin(\theta_c)\cos(\phi_c)\hat{r} + \sin(\theta_c)\sin(\phi_c)\hat{z} + \cos(\phi_c)\hat{\phi} \tag{39}$$

and, the electron velocity $\boldsymbol{v}$ and position $\boldsymbol{r} = r\hat{r}$ denote the electron trajectories.

Description of θ_c and ϕ_c in a cylindrical coordinate system (r, ϕ, z) is given by Figure 2.

Making use of the derived electron trajectories (18), (23) and (25), (26) in (35) up to the order of $\frac{1}{\gamma^2}$, we find,

$$\omega_L t - K_L \boldsymbol{n} \cdot \boldsymbol{r} \approx \frac{K_{\phi L}}{K_{\phi R}} [K_{\phi\Lambda}\phi_0 - \alpha\cos(K_{\phi\Lambda}\phi_0) - \varsigma\sin(2K_{\phi\Lambda}\phi_0)] \tag{40}$$

where

$$K_{\phi R} = \frac{2\gamma^2 K_{\phi\Lambda}}{1 + g_\Lambda^2 + \gamma^2\theta_c^2} = \frac{2\pi}{\phi_R} \tag{41}$$

is the resonant angular wavenumber with ϕ_R being the resonant angular period.

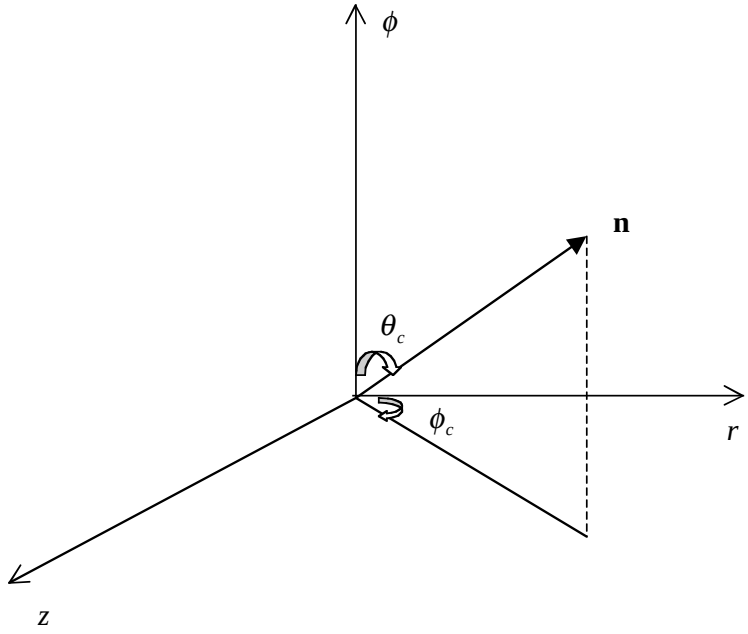

Figure 2. Unit vector in the direction of emission.

Hence, $\lambda_R = r_0\phi_R$ represents the resonant wavelength. θ_c is the half-angle of a cone in which the radiation (Bremsstrahlung) is confined around the direction of electron motion. The parameters α and ς in (40) are given by:

$$\alpha = 2\sqrt{2}\gamma\theta_c \cos(\phi_c)\frac{g_\Lambda}{1+g_\Lambda^2+\gamma^2\theta_c^2} \tag{42}$$

$$\varsigma = \frac{1}{2}\frac{g_\Lambda^2}{1+g_\Lambda^2+\gamma^2\theta_c^2} \tag{43}$$

Study of the electrons' mean phase (linear term) yields an appropriate description of the spontaneous emission as effects of the oscillations around this mean phase are considered in the development of laser field. Expression for the phase associated with the mean motions can be written as:

$$\begin{aligned}\Phi_0 &= -\omega_L t + K_L \boldsymbol{n}\cdot\boldsymbol{r} + nK_{\phi\Lambda}\phi_0 \\ &\approx -\frac{K_{\phi L}}{K_{\phi R}}K_{\phi\Lambda}\phi_0 + nK_{\phi\Lambda}\phi_0\end{aligned} \tag{44}$$

where n is the harmonic number.

The electron mean phase (44) is stationary when,

$$K_{\phi L} = nK_{\phi R}, \quad n = 1, 2, \ldots \tag{45}$$

or

$$\lambda_L = \frac{\lambda_R}{n} \quad n = 1, 2, \ldots \tag{46}$$

In general, for the overall phase resonance we have:

$$K_{\phi L} = nK_{\phi R} + \delta k_\phi \tag{47}$$

where δk_ϕ is a factor representing all the oscillatory effects around resonance.

Limiting our view to the light detection along a circular path ($\theta_c = 0,\ r = r_0$), we obtain from (41), (46),

$$\lambda_L = \lambda_\Lambda \frac{(1 + g_\Lambda^2)}{2n\gamma^2} \tag{48}$$

where λ_Λ is given by (14).

3.3. Electron Dynamics in the Laser Field

To describe the transition toward coherent state, electron's behaviour in the process of interaction with the laser field must be characterized. An important observation is the variation of the electron energy γ in the process of interaction with the electromagnetic field as represented by:

$$\frac{d\gamma}{dt} = \frac{e}{\gamma m^2 c^2} \boldsymbol{E} \cdot \boldsymbol{p} \tag{49}$$

where $\boldsymbol{p} = \gamma m \boldsymbol{v}$ and $\boldsymbol{v}$ is the electron velocity. In (49), $\boldsymbol{E}$ represents the overall electric field which is sum of the laser or radiation field and the static modulating field.

Applying the radiation gauge, the laser field can be assumed to be polarized in the r direction (in cylindrical coordinate system) with a spectrum narrowly distributed about the resonant frequency $\omega_R = \frac{2\pi c}{\lambda_R}$, i.e., narrow lasing linewidth. Hence, the electric field of the laser is given by:

$$\boldsymbol{E}_L = -\frac{\partial \boldsymbol{A}_L}{\partial t} = \sqrt{2} E_L \cos(K_{\phi R}\phi - \omega_R t + \Phi_L)\hat{r} \tag{50}$$

where

$$\boldsymbol{A}_L = \sqrt{2} A_L \sin(K_{\phi R}\phi - \omega_R t + \Phi_L)\hat{r} \tag{51}$$

The laser field amplitude $E_L(A_L)$ and phase Φ_L are slowly varying functions of space and time.

Since electrons do not exchange energy with the static modulating field, there is no contribution from the modulating static field to the variations of electron energy, i.e.,

$$\frac{d\gamma}{dt} = \frac{e}{\gamma m^2 c^2} \boldsymbol{E}_L \cdot p_r \hat{r} \tag{52}$$

The total phase can be expressed as:

$$\Phi = \Phi_0 + \Phi_{osc} \tag{53}$$

with the mean phase,

$$\Phi_0 = K_{\Phi R}\phi_0 - \omega_R t + nK_{\phi\Lambda}\phi_0 \tag{54}$$

and the phase oscillation Φ_{osc}:

$$\Phi_{osc} = \frac{K_{\phi R}}{K_{\phi\Lambda}} \frac{g_\Lambda^2}{4\gamma^2} \sin(2K_{\phi\Lambda}\phi_0) \tag{55}$$

The mean phase (54) is stationary if

$$\gamma^2 = \gamma_{rn}^2 = \frac{K_{\phi R}}{2nK_{\phi\Lambda}}(1 + g_\Lambda^2) \tag{56}$$

In derivation of the resonant energy (56), it is assumed that $nK_{\phi\Lambda} \ll K_{\phi R}$. Accordingly (using (54)),

$$r_0 \frac{d\Phi_0}{dt} = ncK_{\phi\Lambda}\left(1 - \frac{\gamma_{rn}^2}{\gamma^2}\right) \tag{57}$$

Substituting the electric laser field expression (50) and (18) in (52) and averaging over a wiggler period of ϕ_Λ while taking into considerations the orthogonality of Fourier harmonics, we find to the lowest order of $\frac{1}{2nN_\Lambda}(1/\gamma_{rn}^2)$:

$$\begin{aligned} \frac{d\gamma}{dt} &= -\frac{eE_L g_\Lambda}{\gamma_{rn} mc}\left[J_{\frac{(n-1)}{2}}(n\varsigma) - J_{\frac{(n+1)}{2}}(n\varsigma)\right]\sin(\Phi_0 + \Phi_L) \quad n = \text{odd} \\ &= 0 \qquad\qquad\qquad\qquad\qquad\qquad\qquad\qquad\qquad\qquad\qquad\qquad n = \text{even} \end{aligned} \tag{58}$$

where

$$\varsigma = \frac{1}{2}\frac{g_\Lambda^2}{1 + g_\Lambda^2} \tag{59}$$

and $J_n(x)$ is the Bessel function of order n.

Applying the narrow energy width approximation:

$$\frac{\gamma - \gamma_{rn}}{\gamma_{rn}} = \frac{1}{2nN_\Lambda} \ll 1 \tag{60}$$

we obtain the mean position and phase equations as following:

$$r_0 \frac{d\phi_0}{dt} = c\left[1 + \frac{1+\gamma_\Lambda^2}{2\gamma_{rn}^2}\right] \tag{61}$$

$$r_0 \frac{d\Phi_0}{dt} = 2ncK_{\phi\Lambda}\frac{\gamma - \gamma_{rn}}{\gamma_{rn}} \tag{62}$$

Equations (61)–(62) are fundamental equations governing phase motions of electrons in the laser field. Similarly, (58) is an important equation describing the energy variations of relativistic electrons interacting with the laser or radiation field.

3.4. Laser Field Solution

The optical or radiation field can be characterized by applying an electromagnetic theory. Solution of the Helmholtz equation:

$$\nabla^2 \boldsymbol{A} - \frac{1}{c^2}\frac{\partial^2 \boldsymbol{A}}{\partial t^2} = -\mu_0 \boldsymbol{J} \tag{63}$$

in the cylindrical coordinate system (r, ϕ, z) yields the necessary description of the optical field. In (63), $\boldsymbol{A}$ is the optical field vector potential and the current density $\boldsymbol{J}$ is sum of all point currents associated with the individual electrons. Substituting (50)–(51) in (63) and ignoring second derivatives and squares of derivatives of the slowly varying functions A_L and Φ_L, we find:

$$\cos(K_{\phi R}\phi - \omega_R t + \Phi_L)\frac{DE_L}{Dt} - E_L \sin(K_{\phi R}\phi - \omega_R t + \Phi_L)\frac{D\Phi_L}{Dt} = -\frac{1}{2\sqrt{2}\varepsilon_0} J_r \tag{64}$$

where the total derivative is defined by:

$$\frac{D}{Dt} = \frac{c}{r}\frac{\partial}{\partial \phi} + \frac{\partial}{\partial t} \tag{65}$$

The current distribution in (64) is:

$$J_r(\boldsymbol{r}) = \sum_{n=1}^{n_e} e v_r(\boldsymbol{r}_n)\delta(\boldsymbol{r} - \boldsymbol{r}_n) \tag{66}$$

where δ denotes the Dirac delta function and,

$$v_r(\boldsymbol{r}) = \sqrt{2}\frac{c}{\gamma_{rn}} g_\Lambda \sin(K_{\phi\Lambda}\phi) \tag{67}$$

Averaging the partial currents over a volume with an azimuthal dimension large compared to the lasing wavelength (still small compared with the distance over which the amplitude and phase vary significantly), the macroscopic laser field in a phasor form can be represented by:

$$\begin{aligned} \frac{D\overline{E}}{Dt} &= j\frac{g_\Lambda J_e}{2\varepsilon_0\gamma_{rn}}\left[J_{\frac{(n-1)}{2}}(n\varsigma) - J_{\frac{(n+1)}{2}}(n\varsigma)\right]\langle\exp(-j\Phi_0)\rangle \quad n = \text{odd} \\ &= 0 \qquad\qquad n = \text{even} \end{aligned} \tag{68}$$

where J_e is the electron-beam current density and,

$$\overline{E} = E_L \exp(j\Phi_L) \tag{69}$$

In (68), effects of the small oscillations around the mean motion have been averaged over a wiggler period ϕ_Λ.

Similarly, we get for the differential gain:

$$\begin{aligned} \frac{DG}{Dt} &= \frac{\dfrac{D}{Dt}\left(\varepsilon_0 E_L^2\right)}{\varepsilon_0 E_L^2} \\ &= \frac{g_\Lambda J_e}{\varepsilon_0 E_L \gamma_{rn}}\left[J_{\frac{(n-1)}{2}}(n\varsigma) - J_{\frac{(n+1)}{2}}(n\varsigma)\right]\langle\sin(\Phi_0+\Phi_L)\rangle \quad n = \text{odd} \\ &= 0 \qquad\qquad n = \text{even} \end{aligned} \tag{70}$$

The refractive index for the resulting active medium is:

$$\begin{aligned} \frac{n-1}{n} &= \frac{r_0 g_\Lambda J_e}{2c\varepsilon_0 K_{\phi R} E_L \gamma_{rn}}\left[J_{\frac{(n-1)}{2}}(n\varsigma) - J_{\frac{(n+1)}{2}}(n\varsigma)\right]\langle\cos(\Phi_0+\Phi_L)\rangle \\ &\qquad\qquad n = \text{odd} \\ &= 0 \qquad\qquad n = \text{even} \end{aligned} \tag{71}$$

Equation (71) indicates that $(n-1)$ has the same sign as $\langle\cos(\Phi_0+\Phi_L)\rangle$. It is shown [11] that the electrons tend to bunch around the phases $|(\Phi_0+\Phi_L)| < \frac{\pi}{2}$, so $n > 1$. Since the laser medium has a greater refractive index than the surrounding vacuum, the electron beam can confine the light and act as a guiding structure.

Introducing proper dimensionless variables, equations of motions and the Maxwell's equation are solved in the small-signal regime to

obtain the overall gain and the total phase shift during the interaction as follows:

$$G - 1 = 2j_e f(\alpha) \tag{72}$$

$$\Delta\Psi \approx j_e q(\alpha) \tag{73}$$

with $f(\alpha)$ and $q(\alpha)$ given by:

$$f(\alpha) = -\frac{d}{d\alpha}\left[\frac{\sin\left(\frac{\alpha}{2}\right)}{\alpha}\right]^2 \tag{74}$$

$$q(\alpha) = \frac{1}{\alpha^3}\left[\sin(\alpha) - \frac{\alpha}{2}(1+\cos(\alpha))\right] \tag{75}$$

Definition of dimensionless variables, parameters and details of mathematical derivations are included in the Appendix A.

Behaviour of the functions $f(\alpha)$ and $q(\alpha)$ are depicted in Figures 3 and 4.

Figure 3 indicates that the gain function $f(\alpha)$ is largest for positive values of the resonance parameter α. It is also seen that gain vanishes at the resonance $\alpha = 0$. The latter is expected because, at the electron

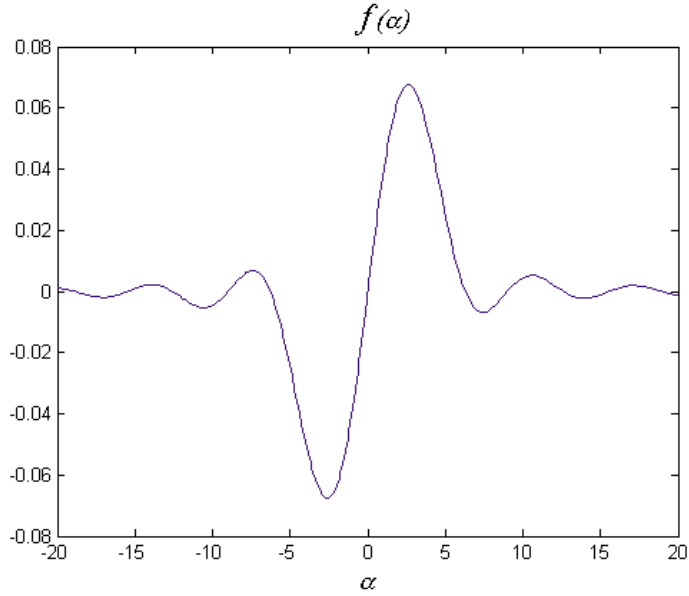

Figure 3. Gain function vs. relative frequency.

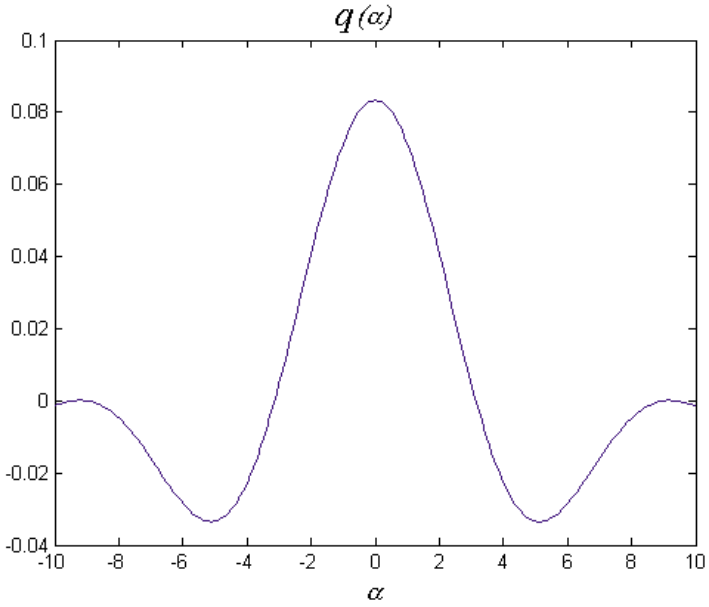

Figure 4. phase function vs. relative frequency.

phase resonance, there would be no electron energy loss to the radiation field.

Inspection of Figure 4 reveals that the overall phase shift is maximum at the resonance and vanishes at the point of maximum gain. The peak value of the gain function occurs at $\alpha = 2.6$, where the function has a value of $f_{\max} = 6.75 \times 10^{-2}$.

3.5. Optical Power Considerations

In order to estimate the extracted optical power, we rewrite the energy conservation relation (A10) as:

$$\frac{d}{d\tau}(2j_e \langle\mu\rangle) + |\zeta|^2 \frac{dG}{d\tau} = 0 \tag{76}$$

Assuming the small signal operation, (76) can be integrated over the interaction space. Doing so when using (72) yields:

$$|\zeta|^2 = -\frac{\langle\Delta\mu\rangle}{f(\alpha)} \tag{77}$$

where $\langle \Delta\mu \rangle$ is related to the power extraction efficiency η by:

$$\eta = -\frac{\langle \Delta\mu \rangle}{4\pi n N_\Lambda} \tag{78}$$

In (77)–(78), $\langle \Delta\mu \rangle$ can be replaced by $\langle \Delta\alpha \rangle$ since we are primarily interested in the power for certain operating wavelength. It can be seen that at the saturation limit where $\langle \Delta\mu \rangle = 2\pi$ and $|\zeta| \approx \pi^2$,

$$\eta = \frac{1}{2nN_\Lambda} \tag{79}$$

gives the *bucket* height.

Amplitude of the electric field is related to the dimensionless field ζ by:

$$|E| = \frac{\gamma_{rn}^2 mc^2 \lambda_\Lambda}{4\pi r_0^2 g_\Lambda e n} \left[J_{\frac{(n-1)}{2}}(n\varsigma) - J_{\frac{(n+1)}{2}}(n\varsigma) \right]^{-1} \frac{|\zeta|}{(2\pi)^2} \tag{80}$$

Using (80) the extracted power per unit cross section of the optical beam can be expressed as:

$$\begin{aligned} P_s &\approx \frac{\gamma_{rn}^2 m^2 c^5 \varepsilon_0 \lambda_\Lambda^2}{16\pi^2 r_0^4 g_\Lambda^2 e^2 n^2} \left[J_{\frac{(n-1)}{2}}(n\varsigma) - J_{\frac{(n+1)}{2}}(n\varsigma) \right]^{-2} \frac{|\zeta|^2}{(2\pi)^4} \quad n = \text{odd} \\ &= 0 \qquad\qquad n = \text{even} \end{aligned} \tag{81}$$

The total optical power using the formula for the effective area of the optical beam [11],

$$A_{eff} \approx L\frac{\lambda_L}{4} \tag{82}$$

where L is the interaction length, becomes:

$$\begin{aligned} P &\approx \frac{\gamma_{rn}^4 m^2 c^5 \varepsilon_0 \lambda_\Lambda^2 \lambda_L}{64\pi^2 r_0^3 g_\Lambda^2 e^2 n^2} \left[J_{\frac{(n-1)}{2}}(n\varsigma) - J_{\frac{(n+1)}{2}}(n\varsigma) \right]^{-2} \frac{|\zeta|^2}{(2\pi)^3} \quad n = \text{odd} \\ &= 0 \qquad\qquad n = \text{even} \end{aligned} \tag{83}$$

The optical power at the saturation limit becomes:

$$\begin{aligned} P &\approx \frac{\gamma_{rn}^4 m^2 c^5 \varepsilon_0 \lambda_\Lambda^2 \lambda_L}{512\pi r_0^3 g_\Lambda^2 e^2 n^2} \left[J_{\frac{(n-1)}{2}}(n\varsigma) - J_{\frac{(n+1)}{2}}(n\varsigma) \right]^{-2} \quad n = \text{odd} \\ &= 0 \qquad\qquad n = \text{even} \end{aligned} \tag{84}$$

To complete the optical power description, we use Madey relation to relate the gain to the spontaneous emission by:

$$G - 1 \approx -\frac{4\pi r_0^2 J_e}{mc^2} \frac{\phi_R^2}{e\gamma_{rn}} \frac{d^2 E_{spon}}{d\Omega d\omega} \tag{85}$$

At this point, we consider a potential design. In this scheme, electrons with the relativistic energy $\gamma = 10(\approx 5Mev)$ are forced to execute circular motion with a cyclotron radius $r_0 = 0.5\,\mathrm{cm}$ under the influence of the cross-fields. A static electric/magnetic field with the angular period $\phi_\Lambda = 0.04\,\mathrm{rad}$ ($N_\Lambda = 157$) and strength $g_\Lambda = 0.01$ is distributed along the circumference of an circle with diameter $d = 2\,\mathrm{cm}$ ($R_0 = 1\,\mathrm{cm}$). The wiggler period observed by electrons is:

$$\lambda_\Lambda = r_0\phi_\Lambda = 200 \quad (\mu\mathrm{m}) \tag{86}$$

Thus, the optical wavelength for the first harmonic is:

$$\lambda_L = \lambda_\Lambda \frac{(1+g_\Lambda^2)}{2\gamma^2} \approx 1\ (\mu\mathrm{m}) \tag{87}$$

Amount of the optical power associated with the first harmonic in the small-signal regime ($|\zeta| = 0 \ldots 0.01$) is shown in Figure 5. It can be seen that even in the very-small signal region the optical power is of the order of tens of milliwatts.

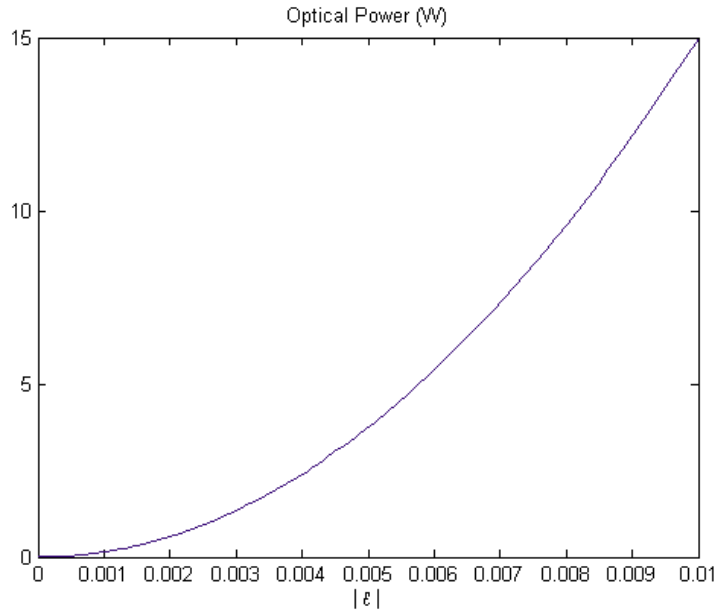

Figure 5. Optical power vs. dimensionless electric field.

4. CONCLUDING REMARKS

Feasibility of the present scheme for high-speed (electro-optical) data communication applications should be investigated in two dimensions. One is the theoretical consideration based on the key characteristics and basic physics of electrons, field and radiation interaction which has been the main focus of present work. Second would be the practical considerations as how to realize the potential device and account for the real operating and model characteristics in the formulations. We discuss the theoretical results and implementation issues in the following categories.

4.1. Theoretical Results and Their Application for Analysis and Design

The theoretical framework here expresses operational characteristics of the electro-optical coupling such as coupled wavelengths, gain and power in terms of model parameters like interaction length, electron current, modulation amplitude and wavelength, and cross fields. Effects of the electron beam quality (e.g., $\left\langle \delta\gamma^2/\gamma_\phi^2 \right\rangle$) are not explicitly included here. Such effects, however, have been included in the dispersion and gain analysis of emission [8] for different beam currents that can identify the respective limitations. Emittance can be measured as a function of beam spot size and wavelength (λ_L) at low current [12]. An electron beam is described through an ellipse equation, $X^T\sigma^{-1}X = 1$, where σ, the beam covariance matrix, determines the area of beam ellipse or emittance. Measurement of σ (even at the end of interaction if the beam propagation matrix is known) would then give the rms emittance. Assuming a Maxwellian distribution for the particles' motion, the emittance is found to be proportional to $(kT)^{1/2}$ [12, 13], where T is the beam temperature . Hence, effects of the beam emittance is somehow included in the analysis of dispersion through inclusion of beam temperature (kT) factor. Furthermore, effects of the electron beam variance are integrated in the coherent formulation of emission and power considerations.

Inspection of the power, energy conservation and efficiency relations (83)–(85), (76), (A10) and (77)–(79) shows that the low power requirement may be translated to low current and/or short interaction length requirements for certain coupled wavelengths and efficiency scenario. This is known in the field of FELs (see Madey relation (85) and spectral influence of the spontaneous emission). In the present circular scenario, reduction of number of wiggles results in a larger angular period ϕ_Λ and hence, a shorter travel radius for

electrons (14). Based on these observations, dispersion characteristics in terms of electron current and energy spread, results of studies on electron beam emittance throughout the interaction in a low current operation [12–14], one concludes that it is more feasible to conserve the quality of electron beam throughout the interaction period in the present scenario.

Making use of the theoretical outcome, operation of the present coupler can be controlled by choosing proper model elements such as beam energy, modulating or input field. An additional degree of tunability is offered here through adjustment of cross-fields. Relations (9)–(10) and (14) indicate the possibility of wavelength tuning by varying the cross-field components. One can also make use of (11) to estimate the wavelength variations due to the change in cyclotron radius during the interaction and devise a compensation scheme based on the control of cross-fields.

4.2. Practical Challenges & Feasibility

Free-electron sources of coherent radiation enjoy diverse and wide spectrum operations with no limitations due to the discrete energy levels existing in conventional lasers. We discuss practical implementation of the present scheme in light of progress in FEL technology through exploration of similarities (or dissimilarities) in challenges.

Similar to FELs, the ring structure here is tunable and can produce a wide variety of pulse formats [1, 15]. Using a storage ring concept [16], high quality electron beam can be achieved. Limitations associated with the electron brightness have been significantly relaxed by virtue of laser switched photocathode electron sources [17, 18]. These photoinjectors can improve the electron beam brightness by two orders of magnitude. As we discussed for the present scenario (operating in Compton scattering regime), however, the electron beam quality and current requirements introduce less stringent limitations considering the current FEL technology achievements and challenges [19–27].

Another attractive feature of the present coupler is the refractive guiding or radiation focusing of the electron beam. This light guiding/confining mechanism which is due to the dielectric response of the electron beam (overall refractive index of greater than 1, see (A14) and (A18), significantly reduces the diffractive losses and the need for guiding mechanisms such as mirrors. Therefore, coupling of the resultant emission to an output device like optical fiber would be practical.

There are challenges particular to this scenario that one should address. Some ideal features of the electro-optical coupler here, such as small size and possibility of beam recycling or continuous beam flow, introduce new challenges. The cross-fields and input modulating fields (typically strong) with required characteristics must be realized in small dimensions. This may represent a challenge from Microsystems point of view. This, however, can be also dealt with by using more attractive alternatives. One potential approach is to apply strong but dense electromagnetic fields for cross or input modulating fields. Described fields are the result of applying the original fields or data to an intermediate scheme. This scheme can be similar to the present coupling scenario (i.e., cascading) [28, 29]. One may also make use of the conventional lasers for this intermediate step.

In order to recycle the electrons or to have continuous beam flow, the required characteristics of the electron beam such as energy and quality must be maintained and refreshed for different input cycles or pulses. Accordingly, energy recovery techniques should be developed to counteract the energy and quality decay. Slippage and lethargy effects in pulsed beam operation of conventional FELs, adversely affect the radiation growth. The slippage and lethargy effects that are due to mismatch between the electron beam velocity (axial) and group velocity of radiation, cause the electron beam pulse lag behind the radiation pulse. This delay in electron response throughout the interaction would eventually cause a distortion of output optical pulse. To prevent the described distortion that could lead to Inter-Symbol Interference (ISI) for data applications, the average slippage time must be made less than the pulse period [1]. For the electro-optical coupler here, the electron beam flow can be assumed to be continuous (not pulsed). The input modulating field, however, is in pulsed or digital format that makes the scenario similar to that of a pulsed electron beam and optical pulse interaction. Therefore, a technique should be devised to make the respective slippage time (when travelling around the ring) small compared to the input pulse period. The cavity tuning to synchronize the electron beam and optical pulses is not a critical factor here (partly because the optical emission is coupled out).

There are challenges particular to the present scenario associated with the convenient assumption of continuous beam flow. As is shown (Section 2.1.), there is a change of electron trajectories associated with the cross-fields' action. In addition, after each interaction cycle or period, there will be a reduction in overall electron beam energy due to interaction and coupling with the optical field, i.e., $\delta\gamma_\phi$. A potential way to compensate for these variations is to devise forward or adaptive schemes for re-adjustment of the cross-field components after each

interaction cycle (9)–(11). There is also a potential to take advantage of these variations for multiplexing purposes (e.g., WDM). As can be seen from (9)–(14) and (46)–(48), after each interaction period and for the same type of input, the optical wavelength is shifted.

Another challenge particular to this scenario is the heat problem. The thermal energy that heats the lasing medium is carried away at near light speed in conventional FELs. Here, however, the energy must be directed out through other mechanisms like heat sinks. One other partial solution could be to refresh the electron beam after a number of cycles.

4.3. Summary

Relativistic free-electron-based emitters offer ideal sources of coherent radiation by virtue of the tunability, short pulse length, synchronize operation, bandwidth and beam quality. These sources are capable of operating over the entire electromagnetic spectrum. FEL is an ideal choice for researchers when there is a need for tunability, high repetition rates and frequency-modulated pulses.

The intention throughout this work has been to exploit the wide-bandwidth and tunable potentials of a scheme based on similar physics for electro-optical data applications. This is not an easy task and many aspects (practical in particular) should be investigated and possibly revisited. Nevertheless, the goal has been to initiate such considerations and respective discussions. On this basis, a theoretical study is done and a feasibility evaluation is performed with the FEL technology as reference frame due to similarity of basic physics and practical challenges. Reported advances of FELs in various dimensions [1, 15–29] such as higher beam and radiation quality, wider tunable range and bandwidth, better pulse format control, migration towards compact and bench top structures further support the feasibility and significance of such electro-optical couplers.

APPENDIX A.

We define the dimensionless variables as:

$$\tau = \frac{1}{r_0}\frac{ct}{2\pi} \tag{A1}$$

$$\xi = \frac{\left(\phi - \frac{1}{r_0}ct\right)}{nN_\Lambda\phi_R} \tag{A2}$$

$$\mu = 4\pi n N_\Lambda \frac{\gamma - \gamma_{rn}}{\gamma_{rn}} \tag{A3}$$

$$\zeta = \frac{8\pi^2 r_0 g_\Lambda e n N_\Lambda}{\gamma_{rn}^2 mc^2}\left[J_{\frac{(n-1)}{2}}(n\varsigma) - J_{\frac{(n+1)}{2}}(n\varsigma)\right]\overline{E} \tag{A4}$$

$$j_e = \frac{(2\pi)^3 r_0^2 g_\Lambda^2 e n N_\Lambda}{\varepsilon_0 \gamma_{rn}^3 mc^3}\left[J_{\frac{(n-1)}{2}}(n\varsigma) - J_{\frac{(n+1)}{2}}(n\varsigma)\right]^2 J_e \tag{A5}$$

Dropping the subscripts associated with the mean motion, equations of motions and the Maxwell's equation are respectively given by:

$$\frac{d\mu}{d\tau} = \mathrm{Re}[j\zeta \exp(j\Phi)] \tag{A6}$$

$$\frac{d\Phi}{d\tau} = \mu \tag{A7}$$

$$\frac{d\xi}{d\tau} = = -1 \tag{A8}$$

$$\frac{d\zeta}{d\tau} = j j_e \langle \exp(-j\Phi)\rangle \tag{A9}$$

The energy conservation, gain and refractive index equations are expressed in terms of the dimensionless variables as:

$$\frac{d}{d\tau}(2j_e \langle\mu\rangle + |\zeta|^2) = 0 \tag{A10}$$

$$\frac{dG}{d\tau} = \frac{2j_e}{|\zeta|}\langle \sin(\Phi + \Phi_L)\rangle \tag{A11}$$

$$\frac{n-1}{n} = \frac{j_e}{2\pi K_{\phi R}|\zeta|}\langle \cos(\Phi + \Phi_L)\rangle \tag{A12}$$

Solving the equations of motion (A6)–(A8) in the small-signal regime by expanding μ, Φ and ξ in power series of ζ_L, we find to the orders of ζ_L ($\ll 1$):

$$\frac{dG}{d\tau} = \frac{j_e}{\alpha^2}[\sin(\alpha\tau) - \alpha\tau\cos(\alpha\tau)] \tag{A13}$$

$$\frac{n-1}{n} = -\frac{j_e}{4\pi K_{\phi R}\alpha^2}[1 - \cos(\alpha\tau) - \alpha\tau\sin(\alpha\tau)] \tag{A14}$$

with

$$\alpha = 2\pi n N_\Lambda\left[2\frac{\gamma - \gamma_{rn}}{\gamma_{rn}} - \frac{k_\phi - K_{\phi R}}{K_{\phi R}}\right] \tag{A15}$$

In the present formulations, the optical field is presented as:

$$\boldsymbol{E}_L = \sqrt{2}E_L \sin(k_\phi\phi - \omega t + \psi_0)\hat{r} \tag{A16}$$

where $k_\phi = r_0 \frac{\omega}{c}$ is the optical wavenumber and, ψ_0 is the initial phase of electrons entering the interaction.

Integrating (A13)–(A14) from the beginning to the end of interaction $\tau = 0$ to $\tau = 1$, one obtains the overall gain and the total phase shift during the interaction as follows:

$$G - 1 = 2j_e f(\alpha) \tag{A17}$$

$$\begin{aligned} \Delta\Psi &= K_{\phi R} \int_0^{2\pi} (n-1) d\phi \\ &\approx 2\pi K_{\phi R} \int_0^1 \frac{n-1}{n} d\tau = j_e q(\alpha) \end{aligned} \tag{A18}$$

Mathematical expressions for $f(\alpha)$ and $q(\alpha)$ are given by:

$$f(\alpha) = -\frac{d}{d\alpha} \left[\frac{\sin\left(\frac{\alpha}{2}\right)}{\alpha} \right]^2 \tag{A19}$$

$$q(\alpha) = \frac{1}{\alpha^3} \left[\sin(\alpha) - \frac{\alpha}{2}(1 + \cos(\alpha)) \right] \tag{A20}$$

REFERENCES

1. O'Shea, P. G. and H. P. Freund, "Free-electron lasers: Status and applications," *Science Magazine*, Vol. 292, 1853–1858, June 2001.
2. Motz, H., "Applications of the radiation from fast electron beams," *J. Appl. Phys.*, Vol. 22, 527, 1951.
3. Motz, H., W. Thon, and R. N. Whitehurst, "Experiments on radiation by fast electron beams," *J. Appl. Phys.*, Vol. 24, 826, 1953.
4. Madey, J. M. J., "Stimulated emission of bremsstrahlung in a periodic magnetic field," *J. Appl. Phys.*, Vol. 42, 1906, 1971.
5. Elias, L. R., W. M. Fairbank, J. M. J. Madey, H. A. Schwettman, and T. I. Smith, "Observation of stimulated emission of radiation by relativistic electrons in a spatially periodic transverse magnetic field," *Phys. Rev. Lett.*, Vol. 36, 717, 1976.
6. Gover, A. and Z. Livni, "Operation regimes of Cerenkov-Smith-Purcell free-electron lasers and T. W. amplifiers," *Opt. Commun.*, Vol. 26, 375, 1978.

7. Report of High-Energy Electron Beam Achievement, FEL Project at Duke, Optics & Photonics News, April 10, 1995.
8. Sabry, R. and S. K. Chaudhuri, "Potential of relativistic electrons and short-wavelength radiation interaction for high-speed electro-optical coupling," *Journal of Electromagnetic Waves and Applications*, Vol. 10, 1237–1261, 1996.
9. Jackson, J. D., *Classical Electrodynamics*, Second Edition, Wiley, New York, NY, 1975.
10. Sabry, R., "Electromagnetic field and high-energy electron beam interaction modelling for high-speed electro-optical applications," Ph.D. Thesis, University of Waterloo, Waterloo, Ontario, Canada, 1996.
11. Brau, C. A., *Free-Electron Lasers, Advances in Electronics and Electron Physics*, Academic Press, San Diego, CA, 1990.
12. Dunham, B. M. and L. S. Cardman, "Emittance measurements for the Illinois/CEBAF polarized electron source," *WPC'95 Proceedings*, 1995.
13. Ross, M. C., N. Phinney, G. Quickfall, H. Shoaee, and J. C. Sheppard, SLAC Report No. 4278, 1987.
14. Edwards D., et al., "The flat beam experiment at the FNAL photoinjector," *Proceedings LINAC2000*.
15. Freund, H. P. and G. R. Neil, *Proc IEEE 87*, 782, 1999.
16. Poole, M., *Synchrotron Radiat. News* Vol. 13, 4, 2000.
17. Sheffield, R. L., *AIP Conference Proceedings 184*, Vol. 2, 1500–1531, 1988.
18. Batchelor, K., et al., *Nucl. Instrum. Methods*, Vol. A318, 372, 1992.
19. Rossbach, J., et al., *Nucl. Instrum. Methods*, Vol. A375, 269, 1996.
20. Milton, S. V., et al., *Science*, Vol. 292, 2037–2041, 2001.
21. O'Shea, P. G., et al., *Phys. Rev. Lett.*, Vol. 71, 3661, 1993.
22. Brau, C. A., et al., *Nucl. Instrum. Methods*, Vol. A318, 38, 1992.
23. Dowell, D. H., et al., *Appl. Phys. Lett.*, Vol. 63, 2035, 1993.
24. Prazeres, R., et al., *Phys. Rev. Lett.*, Vol. 78, 2124, 1987.
25. Hogan, M., et al., *Phys. Rev. Lett.*, Vol. 80, 289, 1998.
26. Nguyen, D. C., et al., *Phys. Rev. Lett.*, Vol. 81, 810, 1998.
27. Tremaine, A., et al., *Phys. Rev. Lett.*, Vol. 81, 5816, 1998.
28. Yu, L. H., et al., *Science*, Vol. 289, 932, 2000.
29. Wu, J., L. H. Yu, et al., *Nucl. Instrum. Methods*, in press.

Ramin Sabry received the B.Sc. degree in electronics and communication engineering from University of Tehran, the M.A.Sc. (electromagnetics and microwaves) and Ph.D. degrees (high-energy electrodynamics and photonics) in electrical engineering from the University of Waterloo, Waterloo, ON, Canada, in 1991 and 1996, respectively. From 1996 to 2002, he was with Ericsson Research where he conducted research on various aspects of wireless communications such as RF components, systems, and radio propagation. He has been an Adjunct Professor with the Electrical and Computer Engineering Department, University of Waterloo. In 2003, he joined Defence R&D in Ottawa where he is currently a scientist. His research interests are in electromagnetics, electro-optics, radio propagation, scattering and diffraction.

Sujeet K. Chaudhuri received the B.E. degree (with honors) in electronics engineering from BITS in 1970, the M.Tech. degree in electrical communication engineering from IIT, Delhi, India, in 1972, and the M.A.Sc. degree in microwave engineering and Ph.D. degree in electromagnetic theory from the University of Manitoba, Winnipeg, MB, Canada, in 1973 and 1977, respectively. In 1977, he joined the University of Waterloo, Waterloo, ON, Canada, where he is currently a Professor in the Electrical and Computer Engineering Department. He was also a Visiting Associate Professor with the Electrical Engineering and Computer Science Department, University of Illinois at Chicago (1981, 1984) and the National University of Singapore (1990–1991). His current research interests are guided-wave/electrooptic structures, planar microwave structures, dielectric resonators (DRs), optical and electromagnetic imaging, and fiberbased broadband networks. Dr. Chaudhuri is a Member of Sigma Xi and the International Scientific Radio Union (URSI) Commission B. He received the 1998 Erskine Fellowship from the University of Canterbury, Canterbury, New Zealand.